A Theoretical Investigation of *P*-Hydroxyphenacyl Caged Phototrigger Compounds: How Water Induces the Photodeprotection and Subsequent Rearrangement Reactions

Xuebo Chen, Chensheng Ma, Wai Ming Kwok, Xiangguo Guan, Yong Du, and David Lee Phillips*

Department of Chemistry, The University of Hong Kong, Pokfulam Road, Hong Kong S.A.R., P. R. China

Received: May 9, 2007; In Final Form: July 17, 2007

Complete active-space self-consistent field (CASSCF) calculations with a (14,11) active space and density functional theory calculations followed by Car−Parrinello molecular dynamic simulations are reported for the *p*-hydroxyphenacyl acetate, diethyl phosphate, and diphenyl phosphate phototrigger compounds. These calculations considered the explicit hydrogen bonding of water molecules to the phototrigger compound and help reveal the role of water in promoting the photodeprotection and subsequent rearrangement reactions for the *p*-hydroxyphenacyl caged phototrigger compounds experimentally observed in the presence of appreciable amounts of water but not observed in neat nonproton solvents like acetonitrile. The 267 nm excitation of the phototrigger compounds leads to an instantaneous population of the $S_3(^1\pi\pi^*)$ state Franck−Condon region, which is followed by an internal conversion deactivation route to the $S_1(^1n\pi^*)$ state via a $^1\pi\pi^*/^1n\pi^*$ vibronic coupling. The shorter lifetime of the $S_1(^1n\pi^*)$ state (∼1 ps) starting from the FC geometry is terminated by a fast intersystem crossing at a $^3\pi\pi^*/^3n\pi^*$ intersection with a structure of mixed $\pi\pi^*/n\pi^*$ excitation in the triplet state. The deprotection reaction is triggered by a proton (or hydrogen atom) transfer assisted by water bridges and emanates from this $\pi\pi^*/n\pi^*$ triplet state intersection. With the departure of the leaving group, the reaction evolves into a water-mediated post-deprotection phase where the spin inversion of *p*QM ($\tilde{X}$, ^3A) leads to a spiroketone in the ground state by a cyclization process that is followed by an attack of water to produce a 1,1′-di-hydroxyl-spiroketone. Finally, the H atom of the hydroxyl in 1,1′-di-hydroxyl-spiroketon transfers back to the *p*-O atom aided by water molecules to generate the *p*-hydroxyphenyl-acetic acid final rearrangement product.

Introduction

Among a wide range of scientists there is much interest in cage compounds and their applications in synthesis and as phototriggers in biological experiments.[1−7] There is increasing attention being given to developing efficient cage compounds for use as phototriggers that can be employed for real-time monitoring of physiological responses in biological systems.[1−7] Removal of the protecting group (or cage) from the protected moiety (such as a biological stimulant) is called deprotection, and in the case of the photon induced removal of the protecting group from the protected moiety in phototriggers this can be thought of as photodeprotection. The *p*-hydroxyphenacyl (*p*HP) protecting group has been of particular interest because of its practical potential as a rapid and efficient "cage" for the release of a variety of biological stimulants.[3−7] Previous work discovered that the photodeprotection reaction of *p*HP caged compounds is highly solvent-dependent and apparently takes place only in aqueous or aqueous containing solutions while the photodeprotection and rearrangement reactions do not occur in neat organic solvents such as acetonitrile (MeCN).[3,7c,e−g,8] In aqueous or aqueous containing solvents, the photodeprotection reaction is accompanied by a photosolvolytic rearrangement of the *p*HP cage into a *p*-hydroxyphenylacetic acid (HPAA) final product (eq 1):

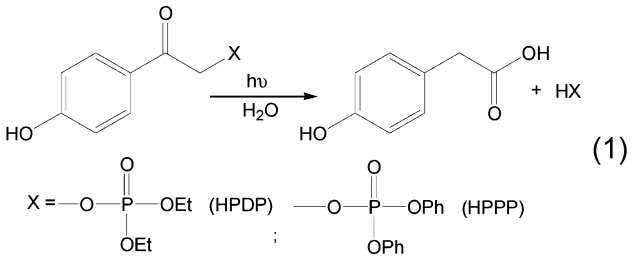

(1)

These observations clearly indicate that water plays a crucial role in both the photodeprotection and photosolvolytic reactions of *p*HP caged compounds.

The products and reaction conditions for *p*HP deprotection have been extensively studied and are fairly well-known.[7c,8,9] However, the reaction mechanism(s) and the key role of water in the photodeprotection and photosolvolytic reactions of *p*HP caged compounds is not well understood. In particular, there is still considerable uncertainty about the events and reactive intermediates involved in the photochemical pathway and how water molecules induce the photodeprotection and photosolvolytic reactions that only occur in the presence of appreciable amounts of water. A number of experimental studies have been done to characterize the intermediates and pathways involved in the photodeprotection and photosolvolytic reactions of *p*HP caged compounds. Givens, Wirz, and co-workers[7c] and Wan and co-workers[8] employed time-resolved transient absorption (TA) spectroscopy to observe several short-lived intermediates

* Author to whom correspondence should be addressed. E-mail: phillips@hkucc.hku.hk. Telephone: 852-2859-2160. Fax: 852-2957-1586.

10.1021/jp073529s CCC: $37.00
Published on Web 09/15/2007

after ultraviolet (~300 nm) excitation of *p*HP caged acetate (HPA) and diethyl phosphate (HPDP) in aqueous containing solvents. However, these studies did not provide an unambiguous interpretation of the data and several different reaction mechanisms have been proposed to account for the photodeprotection and photosolvolytic reactions.[7c,8] We have done further studies employing a combination of femtosecond Kerr gated time-resolved fluorescence (KTRF) and picosecond time-resolved resonance Raman (TR^3) spectroscopy[10] on the HPA and HPDP systems, and this work gave explicit evidence that the triplet state is the reactive precursor for the *p*HP photodeprotection reaction. We have also recently used subpicosecond TA and ps-TR^3 to investigate the HPDP and newly synthesized *p*HP caged diphenyl phosphate (HPPP) phototriggers in H_2O/MeCN mixed solvent systems.[11] TA spectroscopy was employed to examine the solvent decay dynamics of the triplet-state precursor to deprotection, and TR^3 spectroscopy was utilized to follow the formation dynamics of the HPAA rearrangement product in the mixed solvent systems.[11] The faster triplet-state decay with increasing water concentration, the leaving group dependence of the triplet decay, and results in different solvent combinations from these experiments indicated that a water-assisted triplet heterolytic cleavage occurs consistent with site-specific concerted solvation of the hydroxy proton and the leaving group anion through their respective H-bonding with the solvent water molecules. The dynamics of the deprotection and rearrangement reactions indicated these processes occurred sequentially through a solvation complex with contact ion-pair character.[11] An overall reaction mechanism was proposed on the basis of these experimental results for the deprotection and rearrangements reactions for the *p*HP caged phosphate compounds.[11] Comparison of Raman spectra obtained in MeCN solvent and a largely aqueous solvent system for both the ground state and triplet excited-state of several *p*HP caged compounds indicated that there are noticeable explicit hydrogen-bonding effects on these compounds.[11,12] Comparison of the Raman spectra to the vibrational frequencies and structures obtained from density functional theory calculations indicate the hydrogen bonding of the water molecules to the *p*HP compounds leads to significant changes in their structure and properties in both their ground and triplet-excited states.[11,12] It is not yet clear how these explicit hydrogen bonding interactions influence the reaction pathways and photochemistry of *p*HP cage compounds.

While the photodeprotection and photosolvolytic rearrangement reactions of *p*HP cage compounds have been extensively studied by experimental methods over the past decade, there has been little theoretical work done to better understand these reactions[13] and in particular the key role of water in this important photochemistry. Here, we present a theoretical investigation of the photochemistry of selected *p*HP cage compounds in the gas phase and in water complexes that considers the effects of explicit hydrogen bonding on the intermediates and reaction pathways. To our knowledge, this is the first theoretical consideration of explicit hydrogen bonding of water on the excited-state reaction pathways and photochemistry of *p*HP cage compounds. An important question to examine is how do the water molecules promote a direct cleavage of the C−O bond connecting the *p*HP cage and the leaving group.[7c,9] From comparison of the isolated molecule case to that of several water molecules explicitly hydrogen bonded to the *p*HP molecule of interest, we begin to provide new insight into the key role of water in promoting the deprotection reaction that takes place in solvents with appreciable amounts of water. We also explicitly consider the role of water hydrogen bonds in promoting the formation of the HPAA rearrangement product and elucidate the mechanism associated with this reaction that occurs in solvents with significant amounts of water. The results presented here provide new insight into how water hydrogen bonding influences excited-state properties and reaction pathways of the *p*HP photochemistry and enables us to comment on the relevant reactive intermediate(s) involved in the deprotection and rearrangement pathways of *p*HP caged phototrigger compounds. We expect that the excited states of other related aromatic carbonyl compounds and their associated photochemistry in aqueous solvents may also be strongly influenced by explicit hydrogen-bonding effects in a manner similar to that studied here for the of *p*HP caged phototrigger compounds. We anticipate that our modest beginning here to start to explore the role of explicit hydrogen-bonding effects on the excited-state chemistry of *p*HP caged phototrigger compounds will help spur further investigation of the water induced photochemistry of many other interesting aromatic carbonyl (and other related compounds) in aqueous solutions.

Computational Methods

Stationary structures for the *p*-hydroxyphenacyl acetate (HPA) molecule and its complexes with four water molecules (denoted hereafter by HPA-4W) in their seven lowest electronic states (S_0, S_1, S_2, S_3, T_1, T_2, and T_3) have been fully optimized by employing the complete active-space self-consistent field (CASSCF) method. The B3LYP method was also utilized to determine the geometric structures for HPA, HPDP, HPPP and their four water complexes (denoted hereafter as HPA-4W, HPDP-4W, and HPPP-4W) in their ground and triplet states. In this work, the 6-31G* and 6-31G basis sets were chosen and used in the CASSCF and B3LYP calculations. All of the computations reported here were carried out using the Gaussian 03 suite of quantum chemical programs.[14] After preliminary CASSCF calculations using the CAS(10,8)/6-31G level of theory, all of the stationary structures were re-optimized at the CAS(14,11)/6-31G* level of theory. The number of configuration state functions generated in the CASSCF are 1176 for CAS(10,8) and 54615 for CAS(14,11), respectively, in the singlet states (S_0, S_1, S_2, S_3). However, in the triplet states (T_1, T_2, T_3) the numbers increase to become 1512 for CAS(10,8) and 76230 for CAS(14,11), respectively. For the computed equilibrium geometries on the S_0, S_1, S_3, T_1, T_2 surfaces, 14 electrons and 11 orbitals were used in the calculations. These electrons and orbitals originate from the carbonyl C8═O11 and C12═O13 (see the numbering scheme in Figures 1 and 2) π orbitals and C8═O11 π^* orbital, the *para*-hydroxy O7 and O11 nonbonding orbitals, and three π and three π^* orbitals in the aromatic ring. When this (14,11) active space was employed to optimize the structures in the T_3 and the S_2 surfaces, the C8═O11 π^* and O11 nonbonding orbitals were replaced by the C12═O13 antibonding and O13 nonbonding orbitals. Structural optimizations of the surface intersections were performed with the two-root state-averaged CASSCF method. Since the state-averaged calculations are very time consuming and because of the limitations of the available computer memory in our laboratory, the (10,8) active space was used to search for the lowest energy point of the surface crossing seam. To better understand the processes of the photodeprotection and subsequent decay processes, Car−Parrinello molecular dynamics(CPMD) simulations[15] using the atom centered density matrix propagation model (ADMP) were performed on the calculated potential-energy surface (for more details see the following section).

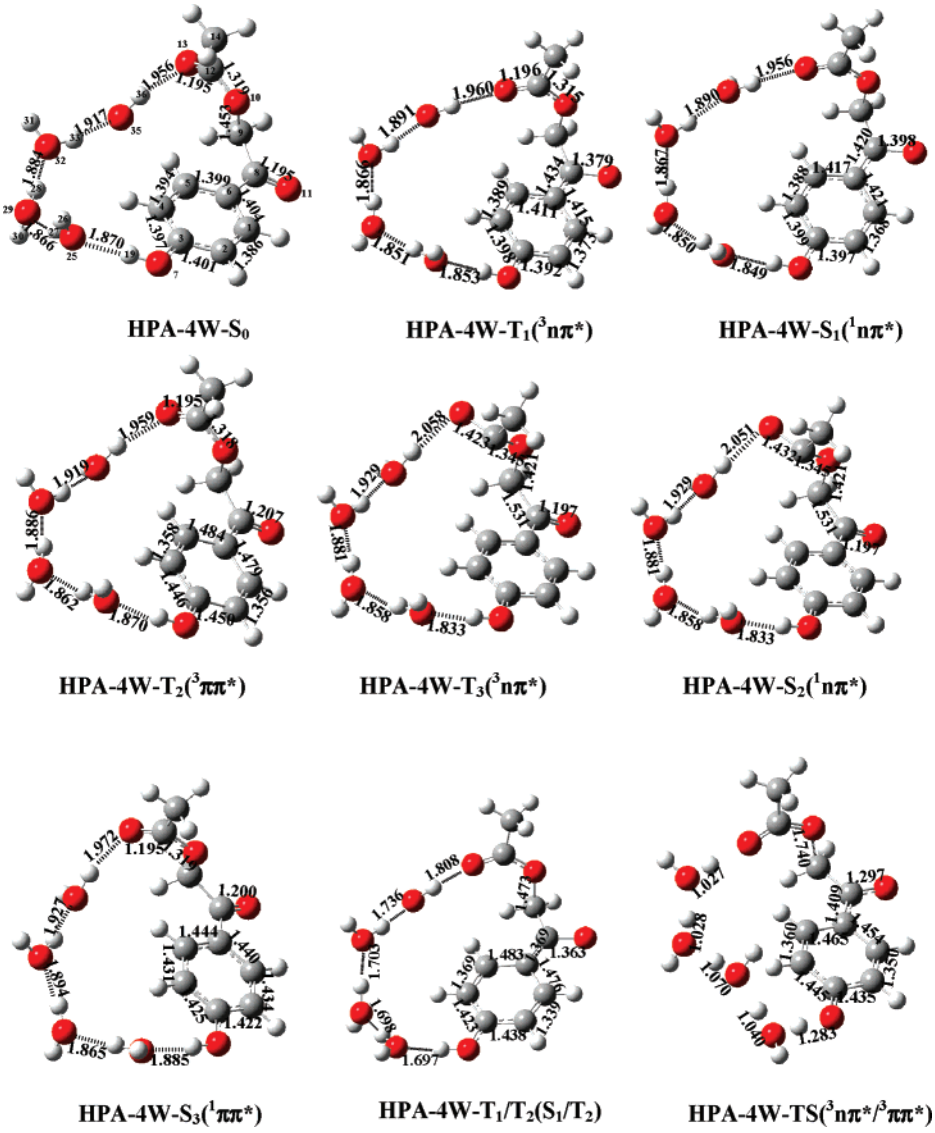

Figure 1. Schematic structures of the stationary and intersection points for *p*-hydroxyphenacyl acetate with $4H_2O$ (HPA-4W) along with selected bond lengths (Å) and the atom labeling scheme for the HPA-4W-S_0 structure.

Results and Discussion

A. The Equilibrium Structures of HPA with $4H_2O$ (HPA-4W) Complexes in the Lowest Seven Electronic States and Their PES Intersections. The departure of the leaving groups and the formation of quinone methides have been proposed to be essential and inevitable steps involved in the mechanistic photochemistry of *p*-hydroxyphenacyl caged phototrigger compounds.[1,7,8] Obviously, the formation of a quinone methide requires the departure of the hydrogen (H atom or proton) from the *para*-hydroxy moiety. Meanwhile, the oxygen atom in the C═O double bond of the OAC (leaving group) provides a good H (atom or proton) acceptor. It is reasonable that the transfer of the H19 (atom or proton) from the *para*-hydroxy moiety to the carbonyl O13 atom could be a primary step in the process of deprotection for HPA and this step is similar to a hydrogen abstraction in a Norrish type II reaction.[16] Since the 19H−O13 distance is in a range between 7.4 and 8.5 Å in the seven minima of HPA, the direct H (atom or proton) transfer is inaccessible in the several lowest electronic states. Here, a mechanism of intramolecular hydrogen or proton transfer aided by water bridges is proposed to gain some insight for the deprotection of *p*-hydroxyphenacyl caged phototrigger compounds. This idea is similar to qualitative proposals made in Wan and coworkers[17−19] in investigations of the mechanistic photochemistry of a variety of hydroxyaromatic compounds in aqueous solution, where a water cluster mediated proton transfer from a hydroxy group is thought to be ultimately responsible for the primary photochemical step. At first, we performed test calculations for *p*-hydroxyphenacyl acetate complexes with a different number of water molecules (HPA-$(H_2O)_{n=1\sim5}$) in the ground state at the B3LYP level of theory. These calculations revealed that the minimum number of water molecules needed for transport of the hydrogen in the water bridge is four. This can saturate the space requirements for the hydrogen abstraction, and the HPA-$(H_2O)_5$ complex does not show an improvement for the interpretation of the mechanism. As a matter of convenience, the *p*-hydroxyphenacyl acetate, diethyl phosphate, and diphenyl phosphate with $4H_2O$ complexes (HPA-4W, HPDP-4W, and HPPP-4W) were employed to be reactant systems for elucidating the deprotection processes aided by water bridges in the calculations presented here.

Figure 1 illustrates the optimized equilibrium structures for *p*-hydroxyphenacyl acetate $4H_2O$ complexes (HPA-4W) in their lowest seven electronic states. The four water molecules are almost equidistantly arranged between the hydroxy H19 and the carbonyl C12═O13 for the HPA-4W complex in the seven

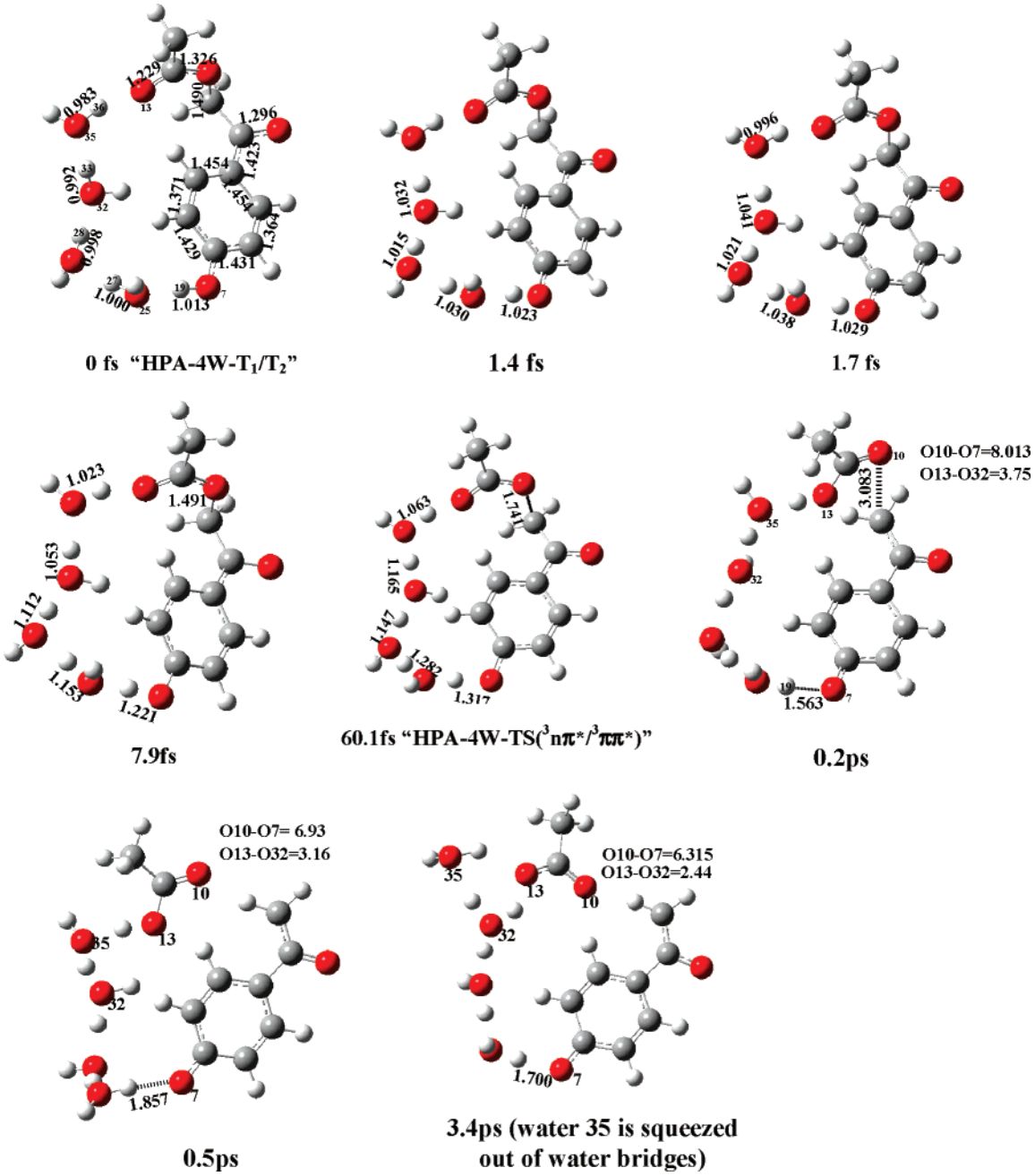

Figure 2. The snapshots along the CPMD trajectory for deprotection of HPA with four water molecules starting from the $^3n\pi^*/^3\pi\pi^*$ intersection are shown.

minima of HPA-4W complexes, and the intervals among the water molecules were found to be in the 1.86∼2.80 Å range. The structural changes from HPA-4W-S_0 to the corresponding lowest six excited states of HPA-4W are similar to those of the HPA molecule without water molecules[13] explicitly added to the reaction system. The following similar structural changes appear with and without water molecules present: (i) an elongated C8−O11 bond for the HPA-4W-$S_1(^1n\pi^*)$, HPA-4W-$T_1(^3n\pi^*)$, HPA-4W-$S_2(^1n\pi^*)$, and HPA-4W-$T_3(^3n\pi^*)$ states; (ii) a diradical configuration with shortened C1−C2 and C4−C5 bonds and elongated C3−C4, C5−C6, C2−C3, and C1−C6 bonds for HPA-4W-$T_2(^3\pi\pi^*)$; (iii) an enlarged benzene ring for the HPA-4W-$S_3(^1\pi\pi^*)$ state.

Although HPA with and without water in the lowest six excited states exhibit the same structural characteristics, their adiabatic energy gaps do not totally mesh at all equilibria (see Table 1).

TABLE 1: The Relative Energies (kcal/mol) for *p*-Hydroxyphenacyl Acetate (HPA) and Four-Water Complexes (HPA-4W) in the Lowest Seven States at CAS(14,11)/6-31g* Level of Theory

HPA-S_0	0.0	0.0	HPA-4W-S_0	0.0
HPA-$T_1(^3n\pi^*)$	73.5	66.9	HPA-4W-$T_1(^3n\pi^*)$	64.9
HPA-$S_1(^1n\pi^*)$	77.3	72.4	HPA-4W-$S_1(^1n\pi^*)$	68.8
HPA-$T_2(^3\pi\pi^*)$	76.1	75.1	HPA-4W-$T_2(^3\pi\pi^*)$	77.4
HPA-$T_3(^3n\pi^*)$	92.7	87.5	HPA-4W-$T_3(^3n\pi^*)$	94.7
HPA-$S_2(^1n\pi^*)$	98.4	92.3	HPA-4W-$S_2(^1n\pi^*)$	99.3
HPA-$S_3(^1\pi\pi^*)$	107.3	107.3	HPA-4W-$S_3(^1\pi\pi^*)$	108.4

The main differences are associated with the energy levels of HPA-4W-$S_1(^1n\pi^*)$ and HPA-4W-$T_1(^3n\pi^*)$ being lowered. Adiabatically, the energy gaps between S_0 and $S_1(^1n\pi^*)$, $T_1(^3n\pi^*)$ were determined to be 68.8 and 64.9 kcal/mol for the $4H_2O$ complexes at the CAS(14,11)/6-31G* level of theory, respectively. These energy gaps between HPA-S_0 and HPA-

$S_1(^1n\pi^*)$, HPA-$T_1(^3n\pi^*)$ were determined to be 77.3 and 73.5 kcal/mol, respectively, at the same computational levels. The HPA-4W-$T_2(^3\pi\pi^*)$ minimum (77.4 kcal/mol) is higher than the HPA-4W-$S_1(^1n\pi^*)$ and HPA-4W-$T_1(^3n\pi^*)$ complexes in energy. The $T_2(^3\pi\pi^*)$ minimum for HPA without water (76.1 kcal/mol) lies sandwiched between the HPA-$T_1(^3n\pi^*)$ (73.5 kcal/mol) and HPA-$S_1(^1n\pi^*)$ (77.3 kcal/mol) states. This finding indicates that the formation of a water complex for HPA leads to energy level inversion of the $n\pi^*$ and $\pi\pi^*$ states and this verifies that the energy ordering of phenyl ketones with a general formula $PhCOCH_2R$ is susceptible to water in agreement with previous experimental observations.[20,21] The strong hydrogen-bonded interaction between the H19 atom and the O atom of water weakens the O7−H19 bond, which in turn enhances the $p-\pi$ conjugation between the O7 atom and the aromatic ring. This effect further strengthens the conjugation interaction between the benzene ring and the C8═O11 carbonyl group and this is responsible for lowering the energy levels of S_1 and T_1 ($n \rightarrow \pi^*$ transition from the O11 nonbonded electron to the π antibonded orbital of C8═O11) for the HPA with water molecules attached. These changes in the conjugation effects are further confirmed by the structural differences observed between HPA-4W-S_0 and HPA-S_0. The O7−H19 bond is elongated from 0.94 Å in HPA-S_0 to 0.96 Å in HPA-4W-S_0 (e.g., a weakened O7−H19 bond), whereas the bond lengths of C3−O7, C6−C8 and C8═O11 are shortened to be 0.014, 0.01, and 0.1 Å, respectively (due to an enhanced conjugation effect), from HPA[13] to HPA with four water molecules in the ground state.

Similar to HPA without water,[13] the $^1n\pi^*$, $^3n\pi^*$, and $^3\pi\pi^*$ states of HPA with water could also intersect in a similar region. The intersection of $^3n\pi^*/^3\pi\pi^*$ (HPA-4W-T_1/T_2) and $^1n\pi^*/^3\pi\pi^*$ (HPA-4W-S_1/T_2) for HPA with $4H_2O$ complexes were optimized by SA-CAS(10,8)/6-31G calculations. The two intersections were confirmed to be indistinguishable in both structure and energy. As illustrated in Figure 2, the C8−O11 bond becomes elongated to 1.363 Å in HPA-4W-T_1/T_2 (HPA-4W-S_1/T_2) and appears to be characteristic of a single bond. Meanwhile, the benzene ring exhibits a cyclohexadienyl character of "four longer (C1−C6, 1.476 Å; C5−C6, 1.483 Å; C3−C4, 1.423 Å; C2−C3, 1.438 Å) and two shorter (C1−C2, 1.339 Å; C4−C5, 1.369 Å) carbon−carbon bonds". These results imply that HPA-4W-T_1/T_2 similarly originates from mixed excitation of $^3n\pi^*$ and $^3\pi\pi^*$. Similar to HPA without water,[13] HPA-4W-T_1/T_2 (HPA-4W-S_1/T_2) is well equilibrated with excitation between the two chromophores of the aromatic ring and the carbonyl moieties. HPA-4W-T_1/T_2 (HPA-4W-S_1/T_2) was found to be located about 5.15 kcal/mol above the HPA-4W-$S_1(^1n\pi^*)$ minimum in energy at the CAS(10,8)/6-31G level of theory.

B. The Water-Mediated Photodeprotection in the $^3n\pi^*$ and $^3\pi\pi^*$ Mixed State. Qualitatively, the H19 transfer and the departure of the −OAC group can proceed along either a stepwise or concerted route. However, numerous attempts for the optimization of the product of the H19 transfer via a four-water molecule-bridge in the triplet state inevitably leads to a structure with C9−O10 bond fission. These findings indicate that H19 transfer via a water chain takes place concomitant with cleavage of the C9−O10 bond in the triplet states, which indicates that stepwise hydrogen transfer occurs with little possibility. A transition state of HPA-4W-TS($^3n\pi^*/3\pi\pi^*$) with simultaneous C9−O10 bond fission and H19 abstraction was found by CAS(14,11)/6-31G* and CAS(10,8)/6-3G optimizations on the triplet pathway of HPA. Following the results of the CAS(10,8)/6-3G calculations, this transition state was confirmed to be connected with the reactants and products in the triplet state by CAS(10,8)/6-3G frequency calculations. The direction of the displacement vectors of the imaginary frequency with a value of 1263.3 cm^{-1} in HPA-4W-TS($^3n\pi^*/^3\pi\pi^*$) points toward simultaneous stretching motions of the C9−O10 bond and H19, H27, H28, H33, and H36 along the four-water-molecule chain. In the direction of the product, the IRC calculations starting from the HPA-4W-TS($^3n\pi^*/^3\pi\pi^*$) lead to the departure of the −OAC group with H36 and the integration of the four water molecules with exchanged hydrogen atoms. To our surprise, the IRC calculations toward the direction of the reactant reaches a structure with an equilibrium of mixed excitations of the aromatic ring and the carbonyl moieties, where the benzene ring appears to have a cyclohexadienyl structural character and the C8−O11 in the carbonyl moiety is simultaneous elongated.

To further ascertain our findings, we re-optimized this concerted transition state of HPA in the triplet state followed by IRC calculations at the B3LYP/6-31G* level of theory. Similarly, the HPA-4W-TS($^3n\pi^*/^3\pi\pi^*$) was confirmed to be connected with a structure with an equilibrium of mixed excitations of the aromatic ring and the carbonyl moieties by the IRC/B3LYP/6-31G* calculations. At the same calculated levels of theory, these chemical events were verified to also occur in the HPDP and HPPP four-water complexes of the triplet-state pathways. Our present calculations provide clear evidence that the photodeprotection of *p*-hydroxyphenacyl caged phototrigger compounds with a four-water-molecule complex (HPA-4W, HPDP-4W, and HPPP-4W) in the triplet state emanates from the T_1/T_2 intersection with $^3n\pi^*$ and $^3\pi\pi^*$ mixed excitation character instead of a "pure" $T_1(^3n\pi^*)$ or $T_2(^3\pi\pi^*)$ minimum. Our calculated results are consistent with and supported by experimental observations and their interpretation. In early spectroscopic studies concerning phenyl alkyl ketones in moderately polar solvents, the overall phosphorescence decay was reported to be nonexponentil, consisting of both a long-lived and a short-lived component.[20d,22−26] Wagner and co-workers suggested that the shorter-lived phosphorescence emanated from an equilibrium mixture of $^3n\pi^*$ and $^3\pi\pi^*$ states for phenyl carbonyl compounds.[27,28] In their photochemical investigations of phenacyl sulfides, Wagner and co-workers thought the population of the $n\pi^*$ and $\pi\pi^*$ transitions were involved in the β-cleavage of the C−S bond.[29] Lim and co-workers suggested that the intermediate lifetimes and anomalous phosphorescence properties arise because of strong mixing of the of aromatic ring and carbonyl moieties excitations.[30] Nakayama and his co-workers also observed a dual exponential phosphorescence decay of benzophenone(BP) in TFE−water and ethanol−water mixtures and attributed the shorter component (3.7 ms) to the lowest triplet state of the free benzophenone with normal $n\pi^*$ character and the long-lived component to the lowest triplet state of a complex BP−H_2O−TFE with mixed $n\pi^*/\pi\pi^*$ character.[31]

As illustrated in Figure 1, The C9−O10 bond length in the transition state of HPA-4W-TS($^3n\pi^*/^3\pi\pi^*$) is 1.740 Å, which is 0.267 Å longer than that in HPA-4W-T_1/T_2. Simultaneously, the H19 atom deviates 1.283 Å from O7 approaching O25 and H27, H28, H33 as well as H36 departing 0.07∼0.11 Å from its original position. In the *p*-quinone methide (*p*QM) moiety of HPA-4W-TS($^3n\pi^*/^3\pi\pi^*$), the C−C bond in the benzene ring appears to have noticeable cyclohexadienyl structural character and the C8−O11 bond exhibits appreciable single-bond character with a bond length of 1.30 Å. These structural features indicate that the structure of HPA-4W-TS($^3n\pi^*/^3\pi\pi^*$) has $^3n\pi^*/$

$^3\pi\pi^*$ mixed character. Similarly, the concerted transition states for the diethyl phosphate (HPDP) and diphenyl phosphate (HPPP) phototriggers with four water molecule complexes were also obtained using B3LYP/6-31G* optimizations (see Supporting Information). The barriers for the triplet-state release for HPA-4W, HPDP-4W, and HPPP-4W are 76.5, 77.6, and 72.7 kcal/mol, respectively, with respect to the corresponding ground state minima (HPA-4W-S_0, HPDP-4W-S_0, and HPPP-4W-S_0) at the B3LYP/6-31G* level of theory. These barriers are not high, which suggests that the concerted deprotection occurs fairly easily from the $^3n\pi^*/^3\pi\pi^*$ intersection. As shown in Figure 5, the triplet state photorelease is initially triggered by a hydrogen abstraction aided by water bridges starting from a $^3n\pi^*/^3\pi\pi^*$ intersection, and the reaction then overcomes the HPA-4W-TS($^3n\pi^*/^3\pi\pi^*$) barrier to produce the diradical of *p*-quinone methide (*p*QM) and the leaving group.

To further explore the details of the dynamics of the triplet state deprotection of HPA with four water molecules, a 3.4 ps triplet Car−Parrinello molecular dynamics (CPMD) simulation at the B3LYP/3-21G level was performed starting from the $^3n\pi^*/^3\pi\pi^*$ intersection. The snapshots along the CPMD trajectory with 0.03 hartree (18.8 kcal/mol) initial kinetic energy are shown in Figure 2. It can be seen from the O7−H19 distance in successive snapshots that the initial motion involves H19 abstraction. The H19 abstraction causes the H27, H28, and H33 atoms to move from their original positions in turn. The change of the H36 position triggers the occurrence of deprotection and evidence for this comes from the geometric structure observed at 7.9 fs: O35−H36 is 1.023 Å; C9−O10 is 1.491 Å (while it is 1.490 Å at 0 fs). In the subsequent times, the distance of C9−O10 is gradually elongated and increased to 1.740 Å at 60.1 fs. Comparing the structural parameters observed at 60.1 fs to those seen for the HPA-4W-TS($^3n\pi^*/^3\pi\pi^*$) transition state (see Figure 2 (60.1 fs structure) and Figure 1, respectively), it was found that they have similar structural parameters in addition to the same 1.740 Å C9−O10 distance. This suggests that the dynamics of HPA with four water molecules from the T_1/T_2 intersection reaches a "transition-state-like" structure when the time evolution reaches about 60.1 fs. Although the HPA-4W reaction system from HPA-4W-T_1/T_2 evolves to HPA-4W-TS($^3n\pi^*/^3\pi\pi^*$) in a very short time, the CPMD simulations reveal that it will take a much longer time for the departure of the leaving group from the *p*-quinone methide (*p*QM) system. As illustrated in Figure 2 and in the Supporting Information (see selected Cartesian coordinates of the CPMD trajectory for the triplet state deprotection; a 3.4 ps dynamics movie is also available from the authors on request), there are a striking trend of structural changes associated with three aspects in the departure phase of the leaving group. First, the O7−H19 distance fluctuates between 1.50∼1.90 Å, and this implies that the water molecules of the water bridges near O7 do not deviate too far. On the other hand, the leaving group (CH_3OCO^-) gradually approaches C3−O7. Finally, the water molecule 35, meanwhile, is "squeezed" out of the water bridges and the leaving group (CH_3OCO^-) approaches water molecule 32. It is expected that the leaving group would "squeeze" water 32, 29, and 25 in turn to achieve its departure journey on the longer time scale. These findings suggest that the departure of the leaving group (CH_3OCO^-) must overcome the resistance of water approaching the C3═O7 bond of the *p*-quinone methide (*p*QM) moiety.

The present CPMD simulations do support our proposed mechanism that the water bridges serve as a "relay" to transport the H atom or proton, which further triggers the triplet state deprotection process starting from the $^3n\pi^*/^3\pi\pi^*$ intersection. The precondition for the occurrence of deprotection is the formation of a water bridge that depends on the water concentration. This is also consistent with our recent experimental observations that the reaction efficiency of the deprotection depends on varying water concentrations for HPA, HPDP, and HPPP in H_2O/MeCN mixed solvents.[10,11] On the other hand, the water molecules hydrogen-bonding network provides significant resistance during the departure phase of the leaving group that is required to complete the deprotection reaction, and the overall full deprotection and formation of the rearrangement products take a substantially longer time and depend on the nature of the leaving group.

Here we would like to briefly address the description of the deprotection being heterolytic or homolytic in nature. A Mulliken charge analysis shows that O10 in HPA-4W-TS($^3n\pi^*/^3\pi\pi^*$) carries a −0.71 charge, while −0.05 charge is distributed to the C9 region at the CAS(10,8)/6-31G level of theory. The charge distributions were also determined to be −0.457, −0.574, and −0.557 for O10 and −0.218, −2.208, and −0.148 for C9 in the HPDP-4W-TS($^3n\pi^*/^3\pi\pi^*$), HPA-4W-TS($^3n\pi^*/^3\pi\pi^*$) and HPPP-4W-TS($^3n\pi^*/^3\pi\pi^*$), structures, respectively, by Mulliken charge analyses at the B3LYP/6-31G* level of theory. These findings suggest that the initial deprotection cleaves the C−O bond to form a contact radical ion pair (CRIP), where the homolytic bond fission is accompanied by electron transfer so the deprotection appears to be a heterolytic cleavage. Our calculations also show that a different leaving group can influence the electron transfer in the process of formation of the contact radical ion pair. Once the contact radical ion pair is formed, the *p*Hp caged compounds can proceed to form solvent separated ion pairs (SSIP) or radical pairs and then finally diffuse to the fully separated ions or radicals or a mixture of these species depending on the solvent polarity, the type of leaving group, and other factors. A similar competitive mechanism of ion-derived versus radical-derived pathways was also proposed by Zimmerman where the outcome is controlled by the type and position of the substituent.[32a,b] Pincock and co-workers suggested that the ratio of ion-derived to radical-derived product is governed by a competition between the electron transfer and the radical reactions with influencing factors including the solvent polarity, the redox potentials of the radical pair, the ease of the deprotection, and so on.[32c,d] Previous observations showed that a *trans*-stilbene/fumaronitrile (CIP) would form a SSIP on about the 100 ps time-scale, and then this would subsequently form the fully separated ions on the 1 ns time-scale.[32e] Similarly, recent work for the aqueous neutralization between pyranine (8-hydroxy-1,3,6-trisulfonate-pyrene or HPTS) and monochloroacetate ($^-OOC-CH_2Cl$ and denoted hereafter as −OAc−Cl) found that the initial photoacid step to make $HPTS^-(D_3O^+)\cdots{}^-O$ occurred faster than 150 fs and then formed $HPTS^-\cdots(D_2O)\cdots$DOAc-Cl with a time constant of about 25 ps that then subsequently formed the fully separated product complex with a time-constant of about 50 ps.[33] The decay of the triplet-state reaction system (or supermolecule) for the HPDP and HPPP phototriggers were observed to decay with time constants of hundreds of ps in ps-TA and ps-TR^3 experiments, and this appears consistent with this decay being due to dissolution of the triplet-state reaction system to free ions (H_3O^+ and the leaving group anion). There is some additional evidence for this view. The dissolution of the *trans*-stilbene/fumaronitrile (SSIP) to he fully separated ions was found to be dependent on molecular structure.[32e] This is similar to our experimental observations that the decay of the triplet-state reaction system

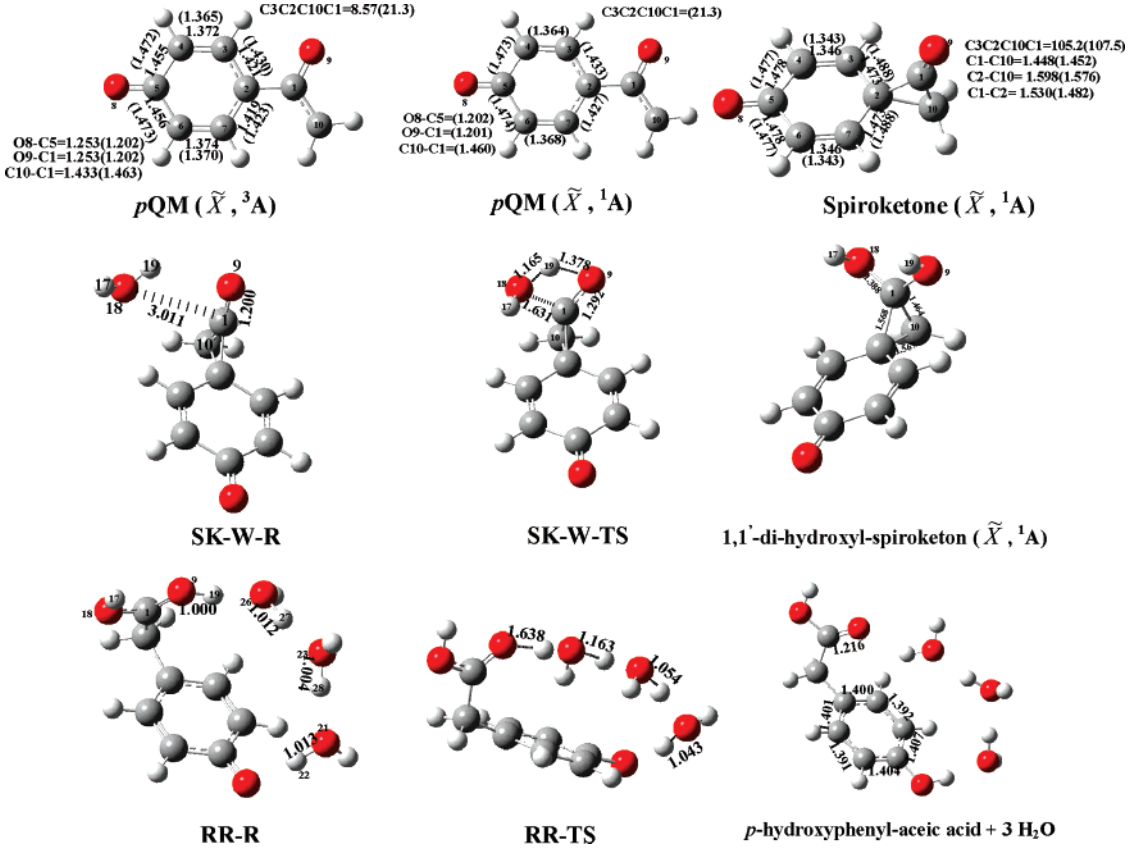

Figure 3. Schematic structures for the stationary points for the processes of water-mediated post-deprotection are shown.

(or supermolecule) for the HPDP and HPPP phototriggers depends on the leaving group structures with a strong correlation of the decay times with the pK_a value of the leaving group anion.[11]

C. The Processes of Water-Mediated Post-Deprotection. *1. Spin Inversion of p-Quinone Methide and the Formation of a Spiroketone.* With the departure of the leaving group, the reaction evolves into the post-deprotection phase in which the triplet state *p*-quinone methide (*p*QM) is the initial reactant. The triplet state *p*-quinone methide was optimized by both CAS-(10,8)/6-31G*, CAS(12,10)/6-31G*, and B3LYP/6-31G* calculations, and its geometric structure is shown in Figure 3 along with selected CAS(12,10)/6-31G* (in parentheses) and B3LYP/6-31G* calculated results. The planar structure of *p*QM in the triplet state was confirmed to be the first-order saddle point with a minor imaginary frequency (36.0 (CAS), 26.8 (B3LYP) cm^{-1}) at the CAS(10,8)/6-31G* and the B3LYP/6-31G* levels of theory and this indicates *p*QM in the triplet state appears to have a quasi-planar structure. An orbital analysis of CAS(10,8)/6-31G* reveals that *p*QM in the triplet state has a diradical configuration where two singly occupied electrons are partitioned mainly on the C2 and C10 regions, respectively. The singlet state *p*-quinone methide ($\tilde{X}$, ^{1}A) was also optimized at both the CAS(10,8)/6-31G* and CAS(12,10)/6-31G* levels of theory. Comparison of the structural parameters between *p*QM ($\tilde{X}$, ^{1}A) and *p*QM ($\tilde{X}$, ^{3}A) (see Figure 3) shows that the *p*QM ($\tilde{X}$, ^{1}A) and *p*QM ($\tilde{X}$, ^{3}A) species are essentially indistinguishable in structure. The energy difference between the *p*QM ($\tilde{X}$, ^{1}A) and *p*QM ($\tilde{X}$, ^{3}A) minima were determined to be 0.9 and 1.0 kcal/mol at the CAS(10,8)/6-31G* and CAS(12,10)/6-31G* levels of theory, respectively. The molecular analysis on the basis of the CASSCF wave function implies that *p*QM ($\tilde{X}$, ^{1}A) is also the configuration of a diradical where two singly occupied electrons are located on the C2 and C10 regions, respectively. Actually, there are very weak mutual interactions between the two singly occupied electrons in *p*QM ($\tilde{X}$, ^{1}A) and *p*QM ($\tilde{X}$, ^{3}A) when the electrons are separated ~2.6 Å (the C10−C2 distance). There are minor differences between the case with the same-spin quantum number (*p*QM ($\tilde{X}$, ^{3}A)) and that with antiparallel spin (*p*QM ($\tilde{X}$, ^{1}A)). This helps to explain why *p*QM ($\tilde{X}$, ^{1}A) and *p*QM ($\tilde{X}$, ^{3}A) are essentially indistinguishable in structure and energy. Meanwhile, these results also imply that the spin inversion easily takes place from the parallel to antiparallel species. We also attempted to optimize the minimum of *P*QM in the singlet state at the B3LYP/6-31G* level of theory. However, the optimizations always lead to a cyclization product in the singlet state that is spiroketone in its ground state. Thus, the likely decay channel for *p*QM ($\tilde{X}$, ^{3}A) is via spin inversion of the singly occupied electron followed by a cyclization to generate a singlet state of *p*QM that is a spiroketone in the ground state. Figure 3 shows some of the structural parameters of spiroketone ($\tilde{X}$, ^{1}A) at the CAS(12,10)/6-31G* (in parentheses) and B3LYP/6-31G* level of theory. The distance between C2 and C10 is shortened from ~2.6 Å in *p*QM ($\tilde{X}$, ^{1}A) to ~1.5 Å in spiroketone ($\tilde{X}$, ^{1}A) that is like a normal C−C single bond. Meanwhile, the three-membered ketone ring is twisted to be ~105° (a dihedral C3C2C10C1 angle) with respect to the quinone ring.

Compared with the quinone ring moiety in *p*QM ($\tilde{X}$, ^{1}A), the most striking changes in the spiroketone ($\tilde{X}$, ^{1}A) are associated with the C2−C3 and C2−C7 bonds. The lengths of these two bonds are elongated to become ~1.47 to 1.48 Å in the spiroketone ($\tilde{X}$, ^{1}A), while they are ~1.42 Å in *p*QM ($\tilde{X}$, ^{1}A). The formation of the C2−C10 bond eliminates the conjugation effect of the singly occupied electron, which is responsible for these structural changes. The spiroketone is 2.2 kcal/mol more stable than *p*QM ($\tilde{X}$, ^{3}A′) in energy at the B3LYP/6-31G* level of theory.

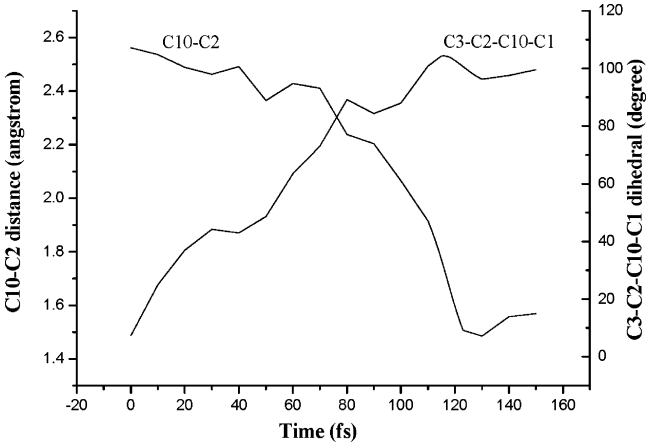

Figure 4. The C3C2C10C1 dihedral angle and the C10−C2 distance as a function of time for the CPMD trajectory for the formation of spiroketone.

To confirm and better understand the processes for the formation of the spiroketone, a single 160 fs CPMD simulation at B3LYP/3-21G level was performed starting from the *p*QM ($\tilde{X}$, ^{3}A) minimum with a zero initial velocity. The MD calculated results were summarized in Figure 4 along with the two parameters of the dihedral C3C2C10C1 angle and the C10−C2 distance. It can be seen from the curve of the CPMD simulations that the C10−C2 distance gradually decreases accompanied by an increase of the C3C2C10C1 dihedral angle. The C10−C2 bond length is 2.54 Å at 10 fs while the C3C2C10C1 dihedral angle is 25.1°. This dihedral increases to 63.5° at 60 fs when the C10−C2 bond becomes 2.43 Å. This bond length is shortened by 0.14 Å from 2.204 Å at 90 fs to 2.066 Å at 100 fs.

Over the same time interval, the C3C2C10C1 dihedral angle increases to 84.4° at 100 fs from 84.4° at 90 fs. The structure from the CPMD simulations at ∼110 fs is very close to that of spiroketone in which the C10−C2 bond length and the C3C2C10C1 dihedral angle are about ∼1.60 Å and ∼100°, respectively. These results imply that the C−C bond has been formed between C10 and C2 when the time reaches ∼110 fs. The present MD simulations not only confirm the proposed mechanistic formation of the spiroketone in which the spin inversion of *p*QM ($\tilde{X}$, ^{3}A) is followed by radical cyclization but also indicate that this process could be achieved in a very short time (110 fs) which is characteristic for a radical cyclization with a low barrier (or possibly no barrier).

2. Hydrolyzation of the Spiroketone. Obviously, the hydrolyzation of the spiroketone starts with the attack of a water molecule, which is a common chemical reaction for carbonyl compounds in aqueous-based media. The B3LYP/6-31G* supermolecule optimization finds a complex structure of the spiroketone with one water molecule that serves as the reactant for the hydrolyzation of the spiroketone in the ground state. As illustrated in Figure 3, the distance between the water molecule and the carbonyl group of the spiroketone is 3.01 Å (the C1−O18 distance) in the supermolecule of water and the spiroketone (SK-W-R). A transition state SK-W-TS was found by the B3LYP/6-31G* calculations and had an imaginary frequency of 1628.6 cm^{-1} that was assigned to be the simultaneous stretching vibration of O9−H19 and C1−O18 on the basis of a frequency analysis. The C1−O18, C1−O9, O9−H19, and H19−O18 distances in SK-W-TS are 1.631, 1.292, 1.378, and 1.165 Å, respectively, at the B3LYP/6-31G* level of theory. With respect to the zero level of SK-W-R, the barrier for the hydrolyzation of the spiroketone is 32.7 kcal/mol at the B3LYP/6-31G* level of theory. The IRC calculations starting from SK-W-TS are confirmed to be connected with the supermolecule SK-W-R in the direction of the reactant. On the other side, the IRC calculations toward the product lead to a 1,1′-di-hydroxyl-spiroketone species. The hydroxyl and H atom of the water molecule attack C1 and O9 of the carbonyl C═O, respectively, to form a 1,1′-di-hydroxyl-spiroketone adduct. The C1−C2 bond length is 1.568 Å in the 1,1′-di-hydroxyl-spiroketone species at the B3LYP/6-31G* level of theory (see Figure 3), and this value is longer than that of 1.464 Å found for the C1−C10 distance. The relatively weaker C1−C2 bond implies that the fission of the C1−C2 bond takes place more easily than that of the C1−C10 bond in the following ring-opening and rearrangement reactions.

3. Water-Assisted Rearrangement Reaction. Since two hydroxyl groups are connected with the same carbon atom of the three-membered ring, there is strong intramolecular repulsion among the groups of the 1,1′-di-hydroxyl-spiroketone species. This inner driving force causes the 1,1′-di-hydroxyl-spiroketone to easily relax to a more stable structure by rearrangement. Qualitatively, the ring-opening and the release of the hydrogen atom from one hydroxyl group could generate an energetically favorable structure of a carbonyl acid. On other hand, the O7 atom of the carbonyl group tends to accept a hydrogen atom in the quinone ring moiety to assist the rebirth of a more stable conformation of the benzene ring with a larger conjugated system. Since the distance between the O atom in the quinone ring and the H atom in the hydroxyl group is ∼ 6.0 Å, it is necessary to seek the help of water molecules to connect these moieties and serve as a "relay" to achieve an intramolecular hydrogen transfer.

A water trimer was introduced to explore a likely water-assisted mechanism for the rearrangement of the 1,1′-di-hydroxyl-spiroketone species. A transition state (RR-TS) was found on the pathway of the rearrangement for the 1,1′-di-hydroxyl-spiroketone water complex in the ground state. The imaginary frequency of RR-TS represents the motions of the coming-and-going for the H19, H22, H27, and H28 atoms along the oxygen chain of O7, O21, O23, O26, O16. The H19, H22, H27, and H28 atoms in RR-TS deviate from the normal O−H bond length, and the approach of the H22 atom toward O7 weakens the C3═O7 double bond. This further causes the delocalization of the π electrons in the whole six-membered ring of the RR-TS transition state. This transition state connects the 1,1′-di-hydroxyl-spiroketone with the three-waters complex (RR-R) in which the three-membered ring has been opened because of the cleavage of the C−C bond. On the other side, the formation of the C22−O7 bond leads to the *p*-hydroxyphenylacetic acid product with three water molecules in the ground state. With respect to the zero level of RR-R, the barrier of RR-TS is 22.8 kcal/mol at the B3LYP/6-31G* level of theory with the zero-point correction included. The loss of a hydrogen atom in the post-deprotection phase is found in the processes of the rearrangement with the structural recurrence of the phenyl ring. In the other moiety, meanwhile, the departure of the H atom causes the formation of the carbonyl C═O double bond which leads to the generation of a carbonyl acid group. Again, the water molecules can act as a "relay" to transport the H atom to return the "borrowed hydrogen" in the processes of the rearrangement reaction.

The mechanism of the water-mediated post-deprotection processes can be summarized as follows: (i) spin inversion of *p*QM ($\tilde{X}$, ^{3}A) followed by a radical cyclization with a low barrier (or possibly with no barrier) to produce a spiroketone in the

ground state; (ii) the spiroketone is attacked by water leading to formation of a 1,1′-di-hydroxyl-spiroketone species; (iii) one H atom of the hydroxyl moiety in the 1,1′-di-hydroxyl-spiroketone species transfers back to the *p*-O atom assisted by a three-water-molecule relay to generate the *p*-hydroxyphenyl-acetic acid final product.

D. Discussion of Mechanistic Aspects. Since the $S_3(^1\pi\pi^*) \leftarrow S_0$ transition adiabatic excitation energy is 103.4 kcal/mol for HPA, the 267 nm (107.1 kcal/mol) photoexcitation of HPA leads to the prompt population of the Franck−Condon region on the $^1\pi\pi^*$ surface. The singlet $\pi \rightarrow ^1\pi^*$ transition is mainly localized on aromatic ring with a deep well and low reactivity (e.g., the fissions of the C−C bonds in the benzene ring are not easy). Thus, IC to the lower singlet surface is the most possible deactivation channel besides radiation processes. Since the $S_2(^1n\pi^*) \leftarrow S_0$ transition for HPA is distributed on the C12−O13 bond of the -OAc group that is far from the aromatic ring, the vibronic interaction between the $S_2(^1n\pi^*)$ and the $S_3(^1\pi\pi^*)$ states is dramatically forbidden. Structurally, the vibronic coupling is expected to occur between the $S_1(^1n\pi^*)$ (excitation of the C8−O11 bond) and the $S_3(^1\pi\pi^*)$ states owing to the direct connection between the carbonyl C8═O11 moiety with the benzene ring. The dual fluorescence phenomena of HPA and HPDP was first observed by our fs-KTRF spectroscopy experiments, and these results confirm the occurrence of vibronic coupling with a very high efficiency between the $S_3(^1\pi\pi^*)$ and $S_1(^1n\pi^*)$ states.[10] The PhCO moiety of HPA in the $S_3(^1\pi\pi^*)$ equilibrium appears to have an almost planar conformation while it exhibits a nonplanar structure in the $S_1(^1n\pi^*)$ minimum. The out-of-plane distortion of the HPA-$S_3(^1\pi\pi^*)$ state causes an increase in the Franck−Condon vibrational overlap factor involving nonplanar vibrations.[34,35] The strong vibronic interaction results in displacement of the nuclear configuration of $S_3(^1\pi\pi^*)$ along an out-of-plane coordinate relaxing to the $S_1(^1n\pi^*)$ state.[36] Our fs-KTRF spectroscopy studies suggest that the lifetimes of HPDP and HPA in the $S_3(^1\pi\pi^*)$ state are around 80 fs including the time of the decay to the $S_3(^1\pi\pi^*)$ minimum from the Franck−Condon region and IC to the $S_1(^1n\pi^*)$ Franck−Condon region via the $^1\pi\pi^*/^1n\pi^*$ vibronic coupling.[10,11]

Considering that the $S_1(^1n\pi^*) \rightarrow T_1(^3n\pi^*)$ process is spin-forbidden, the direct ISC to HPA-$T_1(^3n\pi^*)$ takes place with little probability after the HPA molecule decays to the $S_1(^1n\pi^*)$ Franck−Condon region via the $^1\pi\pi^*/^1n\pi^*$ vibronic coupling. However, a significantly strong first-order spin-orbital interaction causes $S_1(^1n\pi^*) \rightarrow T_2(^3\pi\pi^*)$ ISC to occur with high efficiency.[16] Experimentally, it is well-established that the magnitude of the ISC rate of aromatic ketones is on the order of 10^{11} s^{-1} from a $^1n\pi^*$ state,[37−41] which is at least a 1000-fold faster than those of aliphatic ketones.[42,43] Consistent with Givens' results using the triplet quenching method,[4,7c,e,g] we estimated these ISC rates as being $\sim 5 \times 10^{11}$ s^{-1} for HPA and HPDP in neat as well as H_2O/MeCN mixed solvent from the fs-KTR[3] spectroscopy results.[10] The efficient intersystem crossing (ISC) from $S_1(^1n\pi^*)$ to the triplet manifold is usually explained by the interaction induced by spin−orbit or vibronic coupling. However, the latter reason cannot be applied to all of the cases of aromatic carbonyl compounds by assuming a larger Franck−Condon factor and a large value of the interaction matrix element between the $S_1(^1n\pi^*)$ and the $n\pi^*$ or $\pi\pi^*$ triplet state.[44] The common $S_1(^1n\pi^*)/T(^3\pi\pi^*)/T(^3n\pi^*)$ three surface intersections that are a result of spin−orbital coupling have successfully elucidated the photophysical and photochemical behaviors of a series of aromatic carbonyl compounds.[45−48] Structurally, the HPA molecule appears to have an "enlarged benzene ring" when HPA relaxes to the $S_1(^1n\pi^*)$ Franck−Condon region via the $^1\pi\pi^*/^1n\pi^*$ vibronic coupling and a characteristic of the S_1 state is the stretching of the C8═O10 carbonyl bond. The driving force for stretching the C8═O10 carbonyl bond causes a deformation of the phenyl ring that results in a cyclohexadienyl structural character on the decay pathway of HPA from the S_1 FC geometry. Consequently, the HPA molecule relaxes to the HPA-S_1/T_2 intersection that also coincides with the HPA-T_1/T_2 intersection that has a mixed $\pi\pi^*/n\pi^*$ excitation structure.

To get more dynamics information about this photophysical process, a 50 fs CPMD simulation with a zero initial kinetic energy at B3LYP/3-21G level was performed to ascertain details of the journey for HPA-4W on the $S_1(^1n\pi^*)$ surface. The FC geometry (0 fs) is the same as the HPA-4W $S_3(^1\pi\pi^*)$ minimum in which the C−C bond lengths in the aromatic ring are arranged to be 1.43∼1.44 Å and the C8═O10 has a normal double bond with a bond length of 1.20 Å (see Supporting Information for more details). As time evolves, the C8−O10 bond gradually elongates and the benzene ring deforms from an "enlarged ring" to a cyclohexadienyl character ring. At 12.4 fs, the HPA-4W molecule exhibits the structural characteristics of HPA-4W-T_1/T_2, where the C8−O10 bond length is 1.458 Å and the benzene ring has cyclohexadienyl character [C2−C3 (1.520 Å), C3−C4 (1.458 Å), C5−C6 (1.487 Å), C1−C6 (1.473 Å); and C1−C2 (1.335 Å), C4−C5(1.325 Å)]. These MD calculations not only confirm the decay mechanism of the $S_1(^1n\pi^*)$ surface but indicate that the deactivation for HPA-4W in the S_1 state is a very fast process. This is consistent with our recently experimental investigations that demonstrate the $S_1(^1n\pi^*)$ lifetime of HPA and HPDP were ∼1 ps in H_2O/MeCN.[10]

As discussed above, the transfer of the H19 atom or proton immediately triggers the triplet state deprotection, when the HPA-4W molecule relaxes to the $^3\pi\pi^*/^3n\pi^*$ intersection (HPA-4W-T_1/T_2). The triplet state deprotection takes place easily due to a low barrier to reaction. Our calculations provide compelling evidence that water undoubtedly triggers and participates intimately in the process of the release of the leaving group in the triplet state. Experimentally, these viewpoints are supported by Falvey and co-workers conclusion that H-atom transfer, rather than C−O bond homolysis is the initial photochemical step in the direct photolysis of phenacyl protecting groups studied by transient absorption techniques.[49] A lager isotope effect ($K_{H2O}/K_{D2O} = 2.1$) was found by Mata, Wirz, and Givens in the deprotection of *p*-hydroxyphenacyl caged phototrigger compounds, which indicates the importance of water participation in the photodeprotection reaction.[50] The triplet state deprotection can be roughly divided into thermodynamically (C9−O10 bond fission) and dynamically (departure of the leaving group from the supermolecule system) controlled steps with the dynamically controlled step being the rate-determining step.

Here we briefly discuss the possibility of deprotection from an excited singlet state. A concerted transition state of HPA-4W-$TS_{C-O}(S_1)$ (see the Supporting Information) with simultaneous hydrogen abstraction and C9−O10 bond fission was found by CAS(14,11)/6-31G* optimizations. The most striking structural difference between HPA-4W-$TS_{C-O}(S_1)$ and HPA-4W-$TS_{C-O}(^3\pi\pi^*/^3n\pi^*)$ is associated with the benzene ring moiety. It is a normal aromatic ring in HPA-4W-$TS_{C-O}(S_1)$, while it appears to have a cyclohexadienyl structural character in HPA-4W-$TS_{C-O}(^3\pi\pi^*/^3n\pi^*)$. The structure of the *p*-OHC_6H_4-$COCH_2$ moiety in HPA-4W-$TS_{C-O}(S_1)$ is close to that observed in HPA-$TS_{C-O}(^1n\pi^*)$ in which the C8−O11 bond is significantly elongated. This indicates that HPA-4W-$TS_{C-O}(S_1)$ could

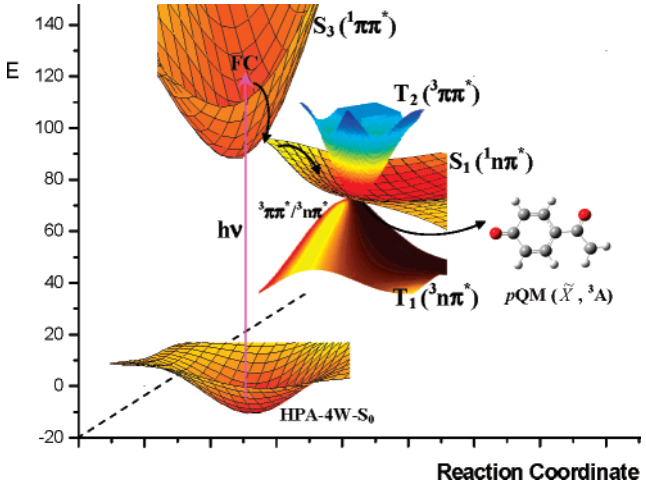

Figure 5. Schematic diagram of the most probable deprotection mechanism upon photoexcitation of HPA irradiated by 267 nm UV light deduced from our present study.

similarly connect with the $S_1(^1n\pi^*)$ minimum on the PES of the HPA with four-water-molecules complex. With respect to the zero-point energy of the HPA-4W-$S_1(^1n\pi^*)$ minimum, the barrier of HPA-4W-$TS_{C-O}(S_1)$ is more than 40.0 kcal/mol and this indicates the deprotection from the $S_1(^1n\pi^*)$ state takes place with great difficulty owing to a high barrier. Actually, the C9−O10 bond fission on the $S_1(^1n\pi^*)$ state for HPA is not easy. As discussed above, the lifetime of $S_1(^1n\pi^*)$ for HPA-4W from the starting FC point is terminated at the $^3\pi\pi^*/^3n\pi^*$ intersection. These results imply that the HPA-4W supermolecule decays to the $S_1(^1n\pi^*)$ minimum with little probability. Considering the high barrier and the unfavorable photophysical process, the possibility of deprotection in an excited singlet state is ruled out. This conclusion has been verified by numerous experimental observations that clearly demonstrate that the triplet state is the precursor to deprotection.[7,10,11] With the departure of the leaving group, the reaction evolves into a water-mediated post-deprotection phase. The spin inversion of *p*QM ($\tilde{X}$, ^{3}A) leads to formation of a spiroketone in the ground state by a cyclization reaction that is followed by attack of water to produce a 1,1′-di-hydroxyl-spiroketone. Finally, the H atom of a hydroxyl group in the 1,1′-di-hydroxyl-spiroketone transfers back to the *p*-O atom via a three-water-molecule relay to generate the *p*-hydroxyphenylacetic acid product.

Conclusion

Complete active-space self-consistent field (CASSCF) calculations using a (14,11) active space and density functional theory (DFT) calculations followed by Car−Parrinello molecular dynamic (CPMD) simulations were presented here for the *p*-hydroxyphenacyl acetate (HPA), diethyl phosphate (HPDP), and diphenyl phosphate (HPPP) phototrigger compounds. The calculations reported here utilized explicit hydrogen bonding of water molecules to the phototrigger compound and help elucidate the role of water in inducing the photodeprotection and subsequent rearrangement reactions for the *p*-hydroxyphenacyl caged phototrigger compounds experimentally observed in the presence of appreciable amounts of water but not observed in neat organic solvents like acetonitrile. As illustrated in Figure 5, the 267 nm excitation of HPA-4W leads to instantaneous population of the $S_3(^1\pi\pi^*)$ state Franck−Condon region, which is followed by IC deactivation to the $S_1(^1n\pi^*)$ state via $^1\pi\pi^*/^1n\pi^*$ vibronic coupling. The shorter lifetime of the $S_1(^1n\pi^*)$ state (∼1 ps) starting from the FC geometry is terminated at a $^3\pi\pi^*/^3n\pi^*$ intersection with a structure of mixed $\pi\pi^*/n\pi^*$ excitation by a fast ISC. The triplet state deprotection is triggered by an intramolecular proton transfer assisted by a water molecule relay (or water bridge) and emanates from this $\pi\pi^*/n\pi^*$ triplet state intersection. The triplet state deprotection could be roughly divided into thermodynamically (C−O bond fission) and dynamically (the leaving of protective group) controlled steps with the latter step being the rate-determining step. The water-mediated post-deprotection phase begins from the spin inversion of *p*QM ($\tilde{X}$, ^{3}A) to form a spiroketone in the ground state by a cyclization process. The carbonyl group of the spiroketone is attacked by water to produce a 1,1′-di-hydroxyl-spiroketone. Finally, the H atom of a hydroxyl group in the 1,1′-di-hydroxyl-spiroketone transfers back to the *p*-O atom via a three-water-molecule relay to form the *p*-hydroxyphenylacetic acid product. The photophysical and photochemical mechanisms of the HPA-4W system can be represented as follows:

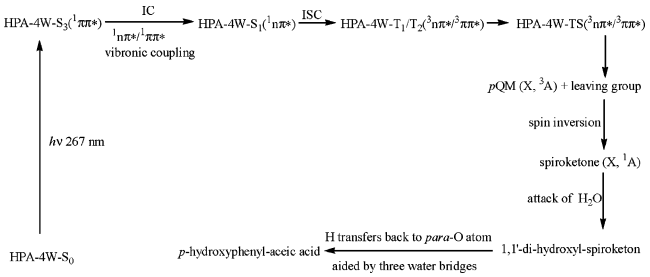

The same photophysical and photochemical mechanisms were predicted for the *p*-hydroxyphenacyl diethyl phosphate (HPDP) and diphenyl phosphate (HPPP) phototrigger compounds. The different leaving groups cause some minor changes of the barrier for photodeprotection in the triplet state for their water complexes. In the present work, we selected water as the helper of hydrogen (or proton) transfer. We do not eliminate that another proton solvent (for instance, CH_3OH) could play the same role in the process of photodeprotection. The further investigations about this issue will be performed in the near future.

Acknowledgment. This research has been supported by grants from the Research Grants Council of Hong Kong (HKU 7108/02P) and (HKU 7036/04P), the award of a Croucher Foundation Senior Research Fellowship (2006-07) from the Croucher Foundation and an Outstanding Researcher Award (2006) from the University of Hong Kong to D.L.P. W.M.K. thanks the University of Hong Kong for the award of a Research Assistant Professorship.

Supporting Information Available: Cartesian coordinates and total energies calculated for the stationary structures on the potential energy surfaces for the photodeprotection for *p*-hydroxyphenacyl acetate with four-water-molecules complexes (HPA-4W); Cartesian coordinates, total energies, and vibrational zero-point energies calculated for the stationary structures on the potential-energy surfaces for the photodeprotection for *p*-hydroxyphenacyl diethyl phosphate and diphenyl phosphate with four water molecules complexes (HPDP-4W and HPPP-4W); selected Cartesian coordinates along the CPMD trajectory for the deprotection of HPA with four water molecules (HPA-4W) starting from the $^3n\pi^*/^3\pi\pi^*$ intersection; selected Cartesian coordinates along the CPMD trajectory for the decay of HPA with four water molecules (HPA-4W) from the S_3 FC geometry to the HPA-4W-S_1/T_2 (HPA-T_1/T_2) intersection; selected Car-

tesian coordinates along the CPMD trajectory for the formation of the spiroketone starting from the *p*QM ($\tilde{X}$, ^3A) species; Cartesian coordinates, total energies, and vibrational zero-point energies calculated for the structures of the stationary points for the processes of water-mediated post-deprotection. This material is available free of charge via the Internet at http://pubs.acs.org.

References and Notes

(1) Goeldner, M.; Givens, R. S. *Dynamics Studies in Biology;* Wiley-VCH Verlag GmbH & Co. KGaA: Weinheim, Germany, 2005.

(2) (a) Pelliccioli, A. P.; Wirz, J. *Photochem. Photobiol. Sci.* **2002**, *1*, 441−458. (b) Bochet, C. G. *J. Chem. Soc., Perkin Trans.* **2002**, *1*, 125−142.

(3) Givens, R. S.; Park, C.-H. *Tetrahedron Lett.* **1996**, *37*, 6259−6262.

(4) Conrad P. G., II; Givens, R. S.; Weber, J. F. W.; Kandler, K. *Org. Lett.* **2000**, *2*, 1545−1547.

(5) (a) Barlos, K.; Gatos, D.; Stauros, K.; Papaphotiv, G.; Schafer, W.; Wenquing, Y. *Tetrahedron Lett.* **1996**, *35*, 6259−6266. (b) Bodi, J.; Sulivargha, H.; Ludanyi, K.; Vekey, K.; Orosz, G. *Tetrahedron Lett.* **1997**, *38*, 3293−3296.

(6) (a) Kandler, K.; Katz, L. C.; Kauer, J. A. *Nat. Neurosci.* **1998**, *1*, 119−123. (b) Specht, A.; Loudwig, S.; Peng, L.; Goeldner, M. *Tetrahedron Lett.* **2002**, *43*, 8947−8950. (c) Du, X.; Frei, H.; Kim, S.-H. *J. Biol. Chem.* **2000**, *275*, 8492−8500.

(7) (a) Zou, K. Y.; Cheley, S.; Givens, R. S.; Bayley, H. *J. Am. Chem. Soc.* **2002**, *124*, 8220. (b) Zou, K. Y.; Miller, W. T.; Givens, R. S.; Bayley, H. *Angew. Chem. Int. Ed.* **2001**, *40*, 3049−3051. (c) Conrad P. G., II; Givens, R. S.; Hellrung, B.; Rajesh, C. S.; Ramseier, M.; Wirz, J. *J. Am. Chem. Soc.* **2000**, *122*, 9346−9347. (d) Geibel, S.; Barth, A.; Amslinger, S.; Jung, A. H.; Burzik, C.; Clarke, R. J.; Givens, R. S.; Fendler, K. *Biophys. J.* **2000**, *79*, 1346−1357. (e) Givens, R. S.; Weber, J. F. W.; Conrad, P. G.; Orosz, G.; Donahue, S. L.; Thayer, S. A. *J. Am. Chem. Soc.* **2000**, *122*, 2687−2697. (f) Givens, R. S.; Jung, A.; Park, C.-H.; Weber, J. F. W.; Bartlett, W. *J. Am. Chem. Soc.* **1997**, *119*, 8369−8370. (g) Park, C.-H.; Givens, R. S. *J. Am. Chem. Soc.* **1997**, *119*, 2453−2463.

(8) Zhang, K.; Corrie, J. E. T.; Munasinghe, V. R. N.; Wan, P. *J. Am. Chem. Soc.* **1999**, *121*, 5625−5632.

(9) Brousmiche, D. W.; Wan, P. *J. Photochem. Photobio. A* **2000**, *130*, 113−118.

(10) Ma, C.; Kwok, W. M.; Chan, W. S.; Zuo, P.; Kan J. T. W.; Toy, P. H.; Phillips, D. L. *J. Am. Chem. Soc.* **2005**, *127*, 1463−1427.

(11) Ma, C.; Kwok, W. M.; Chan, W. S.; Du, Y.; Kan, J. T. W.; Patrick H. T.; Phillips, D. L. *J. Am. Chem. Soc.* **2006**, *128*, 2558−2570.

(12) (a) Chan, W. S.; Ma, C.; Kwok, W. M.; Phillips, D. L. *J. Phys. Chem. A* **2005**, *109*, 3454−3469. (b) Zuo, P.; Ma, C.; Kwok, W. M.; Chan, W. S.; Phillips, D. L. *J. Org. Chem.* **2005**, *70*, 8661−8675.

(13) Chen, X. B.; Ma, C.; Kwok, W. M.; Guan, X.; Du, Y.; Phillips, D. L. *J. Phys. Chem. A* **2006**, *110*, 12406−12413.

(14) Frisch, M. J.; Trucks, G. W.; Schlegel, H. B.; Scuseria, G. E.; Robb, M. A.; Cheeseman, J. R.; Montgomery, J. A., Jr.; Vreven, T.; Kudin, K. N.; Burant, J. C.; Millam, J. M.; Iyengar, S. S.; Tomasi, J.; Barone, V.; Mennucci, B.; Cossi, M.; Scalmani, G.; Rega, N.; Petersson, G. A.; Nakatsuji, H.; Hada, M.; Ehara, M.; Toyota, K.; Fukuda, R.; Hasegawa, J.; Ishida, M.; Nakajima, T.; Honda, Y.; Kitao, O.; Nakai, H.; Klene, M.; Li, X.; Knox, J. E.; Hratchian, H. P.; Cross, J. B.; Bakken, V.; Adamo, C.; Jaramillo, J.; Gomperts, R.; Stratmann, R. E.; Yazyev, O.; Austin, A. J.; Cammi, R.; Pomelli, C.; Ochterski, J. W.; Ayala, P. Y.; Morokuma, K.; Voth, G. A.; Salvador, P.; Dannenberg, J. J.; Zakrzewski, V. G.; Dapprich, S.; Daniels, A. D.; Strain, M. C.; Farkas, O.; Malick, D. K.; Rabuck, A. D.; Raghavachari, K.; Foresman, J. B.; Ortiz, J. V.; Cui, Q.; Baboul, A. G.; Clifford, S.; Cioslowski, J.; Stefanov, B. B.; Liu, G.; Liashenko, A.; Piskorz, P.; Komaromi, I.; Martin, R. L.; Fox, D. J.; Keith, T.; Al-Laham, M. A.; Peng, C. Y.; Nanayakkara, A.; Challacombe, M.; Gill, P. M. W.; Johnson, B.; Chen, W.; Wong, M. W.; Gonzalez, C.; Pople, J. A. *Gaussian 03*, revision C.02; Gaussian, Inc.: Wallingford, CT, 2004.

(15) Car, R.; Parrinello, M. *Phys. Rev. Lett.* **1985**, *55*, 2471−2474.

(16) Turro, N. J. *Modern Molecular Photochemistry*; University Science Books: Sausalito, CA, 1991.

(17) Fischer, M.; Wan, P. *J. Am. Chem. Soc.* **1998**, *120*, 2680−2681.

(18) Diao, L.; Yang, C.; Wan, P. *J. Am. Chem. Soc.* **1995**, *117*, 5369−5370.

(19) Shi, Y.; Wan, P. *J. Chem. Soc., Chem. Commun.* **1997**, 273−274.

(20) (a) Yang, N. C.; Dusenbery, R. *J. Am. Chem. Soc.* **1968**, *90*, 5899−5900. (b) Yang, N. C.; McClure, D. S.; Murov, S. L.; Houser, J. J.; Dusenbery, R. *J. Am. Chem. Soc.* **1967**, *89*, 5466−5468. (c) Long, M. E.; Lim, E. C. *Chem. Phys. Lett.* **1973**, *20*, 413−418. (d) Rauh, R. D.; Leermakers, P. A. *J. Am. Chem. Soc.* **1968**, *90*, 2246−2249. (e)Van Bergen, T. J.; Kellogg, R. M. *J. Am. Chem. Soc.* **1972**, *94*, 8451−8471.

(21) (a) Wagner, P. J. *Acc. Chem. Res.* **1971**, *4*, 168−177. (b) Wagner, P. J. *J. Am. Chem. Soc.* **1967**, *89*, 5898−5901. (c) Wagner, P. J.; Kemppainen, A. E. *J. Am. Chem. Soc.* **1968**, *90*, 5898−5899. (d) Wagner, P., J.; Truman, R. J.; Sciano, J. C. *J. Am. Chem. Soc.* **1985**, *107*, 7093−7097.

(22) Yang, N. C.; Murov, S. L. *J. Chem. Phys.* **1966**, *45*, 4358−4358.

(23) Lamola, A. A. *J. Chem. Phys.* **1967**, *47*, 4810−4816.

(24) Case, W. A.; Kearns, D. R. *J. Chem. Phys.* **1970**, *52*, 2175−2191.

(25) Yang, N. C.; Dusenbery, R. *Mol. Photochem.* **1969**, *1*, 159−171.

(26) Griffin, R. N. *Photochem. Photobiol* **1968**, *7*, 159−173.

(27) Wagner, P. J.; May, M. J.; Haug, A.; Graber, D. R. *J. Am. Chem. Soc.* **1970**, *92*, 5269−5270.

(28) Wagner, P. J.; Nakahira, T. *J. Am. Chem. Soc.* **1973**, *95*, 8474−8475.

(29) Wagner, P. J; Lindstrom, M. J. *J. Am. Chem. Soc.* **1987**, *109*, 3062−3067.

(30) Li, Y. H.; Lim, E. C. *Chem. Phys. Lett.* **1970**, *7*, 15−18.

(31) Nakayama, T.; Sakurai, K.; Hamanaue, K. *J. Chem. Soc., Faraday Trans.* **1991**, *87*, 1509−1512.

(32) (a) Zimmerman, H. E. *J. Am. Chem. Soc.* **1995**, *117*, 8988-8991. (b) Zimmerman, H. E. *J. Phys. Chem.* **1998**, *102*, 5616−5621. (c) Pincock, J. A. *Acc. Chem. Res.* **1997**, *30*, 43−49. (d) Hilborn, J. W. M. E.; Pincock, J. A.; Wedge, P. J. *J. Am. Chem. Soc.* **1994**, *116*, 3337−3346. (e) Peters, K. S.; Lee, J. *J. Am. Chem. Soc.* **1993**, *115*, 3643−3646.

(33) Mohammed, O. F.; Pines, D.; Dreyer, J.; Pines, E.; Nibbering, E. T. *Science* **2005**, *310*, 83−86.

(34) Lim, E. C. *Molecular Luminescence;* Benjamin: New York, 1969; p 469.

(35) Li, Y. H.; Lim, E. C. *Chem. Phys. Lett.* **1969**, *4*, 25-26.

(36) Lim, E. C.; Li, Y. H.; Li, R. *J. Chem. Phys.* **1970**, *53*, 2443−2448.

(37) Anderson, R. W.; Hochstrasser, R. M.; Lutz, H.; Scott, G. W. *J. Chem. Phys.* **1974**, *61*, 2500−2506.

(38) Morris, J. M.; Williams, D. F. *Chem. Phys. Lett.* **1974**, *25*, 312−314.

(39) Matsumoto, T.; Sato, M.; Hiroyama, S. *Chem. Phys. Lett.* **1972**, *13*, 13−15.

(40) El-Sayed, M. A. *J. Chem. Phys.* **1964**, *41*, 2462−2467.

(41) El-Sayed, M. A.; Leyerle, R. *J. Chem. Phys.* **1975**, *62*, 1579−1580.

(42) Halpern, A.; Ware, W. R. *J. Chem. Phys.* **1970**, *53*, 1969−1977.

(43) Hansen, D. A.; Lee, K. C. *J. Chem. Phys.* **1975**, *62*, 183−189.

(44) Ohmori, N.; Suzuki, T.; Ito, M. *J. Phys. Chem.* **1988**, *92*, 1086−1093.

(45) Fang, W. H.; Phillips, D. L. *ChemPhysChem*. **2002**, *3*, 889−892.

(46) Fang, W. H.; Phillips, D. L. J. *Theor. Comput. Chem*. **2003**, *2*, 23−31.

(47) He, H. Y.; Fang, W. H.; Phillips, D. L *J. Phys. Chem. A* **2004**, *108*, 5386−5392.

(48) Chen, X. B.; Fang, W. H. *J. Am. Chem. Soc.* **2004**, *126*, 8976−8970.

(49) Banerjee, A.; Falvey, D. E. *J. Am. Chem. Soc.* **1998**, *120*, 2965−2966.

(50) Givens, R. S.; Lee, J. I. *J. Photosci.* **2003**, *10*, 37−48.